analytical chemistry

Article

Cite This: *Anal. Chem.* 2018, 90, 8196−8201

pubs.acs.org/ac

Antibody-Mediated Small Molecule Detection Using Programmable DNA-Switches

Marianna Rossetti,[†] Rudy Ippodrino,[‡] Bruna Marini,[‡] Giuseppe Palleschi,[†] and Alessandro Porchetta*[,†]

[†]Department of Chemical Sciences and Technologies, University of Rome Tor Vergata, Via della Ricerca Scientifica 1, 00133 Rome, Italy

[‡]Ulisse BioMed S.r.l., Area Science Park, 34149 Trieste, Italy

Supporting Information

ABSTRACT: The development of rapid, cost-effective, and single-step methods for the detection of small molecules is crucial for improving the quality and efficiency of many applications ranging from life science to environmental analysis. Unfortunately, current methodologies still require multiple complex, time-consuming washing and incubation steps, which limit their applicability. In this work we present a competitive DNA-based platform that makes use of both programmable DNA-switches and antibodies to detect small target molecules. The strategy exploits both the advantages of proximity-based methods and structure-switching DNA-probes. The platform is modular and versatile and it can potentially be applied for the detection of any small target molecule that can be conjugated to a nucleic acid sequence. Here the rational design of programmable DNA-switches is discussed, and the sensitive, rapid, and single-step detection of different environmentally relevant small target molecules is demonstrated.

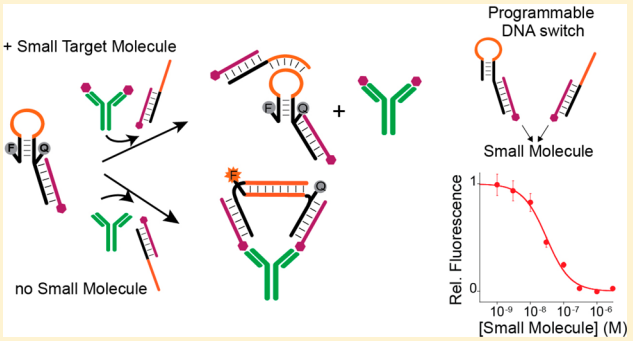

Rapid, cost-effective, single-step assays for the quantitative detection of small molecules are very attractive for many applications including drug discovery,[1,2] metabolomics,[3,4] food analysis,[5] environmental monitoring,[6,7] and clinical diagnosis.[8−10] Although spectroscopic and mass spectrometric techniques have achieved impressive results,[11−13] these methods are generally time-consuming and cumbersome. Recently, the emergence of high throughput "omics" techniques has radically changed the ability to detect, identify, and characterize small molecules, especially since omics approached the single-cell level.[14,15] Nevertheless, also these emerging methods require large equipment (i.e., mass spectrometry, capillary electrophoresis) and trained operators. Enzyme-linked immunosorbent assays (ELISA) represent an alternative, showing several advantages such as impressive sensitivity, specificity, and easy standardization. However, multiple separation and washing steps make the analytical procedure rather time-consuming and laboratory intensive. Therefore, routine ELISA assays utilizing large equipment and multistep analysis are not easily applicable for point-of-care testing (POCT), as well as in the field for environmental and food analysis.

In an attempt to overcome these limitations, a common strategy has been to miniaturize state-of-the-art analytical work flows (i.e., immunoassays) using microfluidics[16−18] and lab-on-a-chip biosensors.[19,20] Among them, detection platforms that employ a nucleic acid aptamer as signaling receptor have been implemented into a plethora of optical,[18,21−25] electrochemical,[26−32] and colorimetric[33−36] formats for the detection of small molecules. Aptamers can be developed against nearly any desired target through in vitro selection, and many strategies have been explored to optimize their analytical performance.[37−39] However, many synthetic nucleic acid aptamers bind small molecules with low affinity making them unsuitable for sensing applications;[40,41] and only a limited number of small-molecule-binding aptamers that robustly function in complex environments have become effective[42,43] and implemented in artificial devices.[44−46] As an alternative, small molecules have been also detected through DNA-based assays[47,48] and proximity ligation assays that take advantage of the proximity effect caused by colocalization of antibody-labeled DNA probes.[49,50] Although this assay is homogeneous and the high sensitivity outperforms ELISA test, even with much smaller sample volumes, the use of qPCR prevents its use in on-site applications.

Motivated by the above limitations, we propose here an innovative strategy that couples the advantages of programmable structure-switching DNA-based probes with those of proximity-based methods for the detection of small target analytes. Specifically, we developed a competitive fluorescence single-step detection of environmentally relevant small target analytes.

Received: April 9, 2018
Accepted: June 6, 2018
Published: June 6, 2018

DOI: 10.1021/acs.analchem.8b01584
Anal. Chem. 2018, 90, 8196−8201

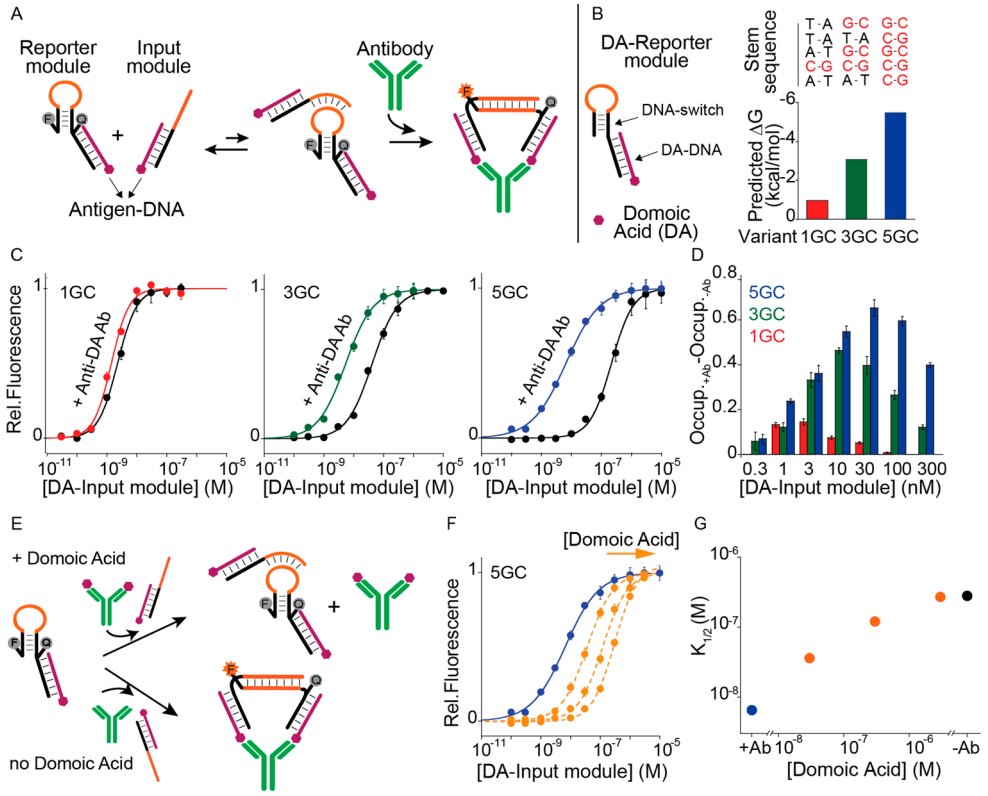

Figure 1. Rational design of programmable DNA-switches for the detection of small molecules. (A) A synthetic stem-loop DNA-probe (DNA-switch) modified with AlexaFluor680/BHQ-2 FRET pair flanked by a 20-base single-stranded tail hybridizes with a complementary DNA strand (Antigen-DNA, purple strand) to generate a reporter module. Antigen-DNA is a nucleic acid sequence conjugated with a specific recognition element (i.e., antigen, purple hexagon). The input module is composed of the same Antigen-DNA that is able to hybridize with a complementary portion of the DNA input strand (black portion). The input strand also contains a 15-base sequence complementary to the loop of DNA-switch (orange portion). In the presence of the specific antibody, the reporter and input modules come into close proximity, which results in their efficient hybridization. (B) To generate domoic acid-reporter module (DA-reporter module), we employ a domoic acid-labeled DNA sequence (DA-DNA) that is complementary to the tail of the DNA-switch. We designed different DNA-reporter modules each one containing a variant of DNA-switch that differs in the GC content of the 5-base stem. (C) Binding affinity experiments between three variants of DA-reporter module (10 nM) and the DA-input module in the presence (i.e., 100 nM, colored curves) and in the absence (black curves) of anti-DA IgG antibodies. (D) Difference of antibody binding sites occupancy for three variants of DA-reporter module (10 nM) at different concentrations of DA-input module. (E) Schematic representation of competitive antibody-mediated DNA-based assay to detect small molecules. In the absence of the specific small target molecule (bottom), the DA-reporter module and the DA-input module bind to the same antibody and their relative affinity binding increase. This ultimately generates a high fluorescence signal. In the presence of domoic acid, competition with domoic acid labeled to the DA-DNA strand prevents the binding of the DA-reporter and DA-input module to anti-DA antibodies resulting in lower fluorescence emission. (F) In the presence of a fixed concentration of domoic acid (i.e., 30, 300 nM, and 3 μM) and anti-DA antibodies (100 nM) the affinity binding of the DA-input module for the DA-reporter module decreases as a function of free domoic acid in solution (orange curves). (G) $K_{1/2}$ values for the binding of the DA-reporter module (1 nM) to the DA-input module depends on the concentration of domoic acid in solution. All the reported values represent the average of at least three measurements, and error bars reflect standard deviations. All the experiments were performed in 100 μL solution of NaH_2PO_4 (50 mM) + NaCl (150 mM) at pH 7.0 at 35 °C.

EXPERIMENTAL SECTION

Reagents. Anti-Domoic Acid IgG antibody was purchased from Inycom Biotech, Spain (mouse monoclonal anti-DA Ab). Anti-2,4-dinitrophenol IgE antibody was purchased from Sigma-Aldrich, St Louis, Missouri (mouse monoclonal anti-DNP Ab). Antibodies were aliquoted and stored at 4 °C for immediate use or at −20 °C for long-term storage. NaCl and NaH_2PO_4 were purchased from Sigma-Aldrich, St Louis, Missouri and used without any further purifications. Non-labeled and dual-labeled oligonucleotides (HPLC purified) used in this work were purchased from IBA GmBH (Gottingen, Germany). Stem-loop DNA-probes (DNA-switch) were terminally modified with AlexaFluor 680 (AF680) and internally with Black Hole Quencher 2 (BHQ2). Single stranded DNA sequence terminally conjugated with Domoic Acid (DA) was purchased from Bio-Synthesis, Inc. (Lewisville, Texas). DNP-labeled DNA sequences were purchased from IBA GmBH (Gottingen, Germany). The sequences and modification schemes of the oligonucleotide are reported here below.

DNA Sequences. *DNA-Switch. Variant 1GC.* 5′-T-(Alexa680)ACATT *ATCTAATGGTGAGTC*AATGT T-(BHQ2) **CT AGAATAAAACGCCACTG**-3′

Variant 3GC. 5′-T(Alexa680) ACGTG *ATCTAATGGT-GAGTC* CACGT T(BHQ2) **CT AGAATAAAACGCCACTG**-3′

Variant 5GC. 5′-T(Alexa680) CCGCG *ATCTAATGGT-GAGTC* CGCGG T(BHQ2) **CT AGAATAAAAC-GCCACTG**-3′

In the above-reported sequences the underlined bases represent the stem portion, while the italic bases represent the loop portion. Bold bases represent a portion that is

DOI: 10.1021/acs.analchem.8b01584
Anal. Chem. 2018, 90, 8196−8201

complementary to the Antigen-DNA strand (DA- and DNP-labeled DNA strand).

Input Strand. 5′- *GACTCACCATTAGAT* ATTTTTTTTT-TTTTTTTCTT **AGAATAAAACGCCACTG**-3′

Here italic bases represent the portion complementary to the loop of DNA-switch sequences. The underlined bases represent the linker introduced to enhance flexibility of the system. Bold bases represent a nucleic acid portion complementary to Antigen-DNA strand.

Antigen-DNA Strands. Domoic Acid-Labeled DNA Strand (DA-DNA). 5′- (DA) CAG TGG CGT TTT ATT CTT GT-3′

DNP-Labeled DNA Strand (DNP-DNA). 5′-(DNP) TTT TTT TCA GTG GCG TTT TAT TCT-3′

Marine Water Samples. Marine water samples were filtered through a 0.4 μm cartridge filter (Whatman 25 mm cellulose acetate membrane) and stored in a polyethylene bottle at 4 °C.

Fluorescence Measurements. All fluorescence measurements were conducted in 100 μL solution of Na_2HPO_4 (50 mM) + NaCl (150 mM) at pH 7.0 at 35 °C. Steady state fluorescence measurements were obtained using a Cary Eclipse Fluorimeter with excitation at 680 (±5) nm and acquisition from 700 nm to 720 (±10) nm. All the fluorescence experiments were performed in quartz cuvettes (100 μL). The intensity of the fluorescence emission was measured at a fixed emission wavelength (λ_{em} = 702 nm). Binding curves reported in Figures 1C and S1 of the Supportiong Information (SI) were obtained at fixed concentration of DA-reporter module (10 nM) in the absence and in the presence of a fixed concentration of anti-DA IgG antibodies (100 nM) by sequentially increasing the concentration of the DA-input module (V_{added} = 5 μL) and taking in account the relative increase of the volume. Binding curves (in orange) reported in Figures 1F and S2 were obtained at fixed concentration of DA-reporter module (10 nM) and anti-DA IgG antibodies (100 nM) and in the presence of a fixed concentration of free DA (i.e., 30 nM, 300 nM, 3 μM) by sequentially increasing the concentration of the DA-input module (V_{added} = 5 μL). Binding curves reported in Figures S4 and S5 were obtained by sequentially increasing the concentration of anti-DA IgG antibodies (V_{added} = 5 μL) to a solution containing a fixed concentration of the reporter (10 nM) and input modules (10 nM). Competitive binding curves reported in Figures 2A, 3A, and S7 were obtained by adding a fixed concentration of the reporter and input modules (10 nM and 10 nM, respectively) to a solution (100 μL) containing the specific antibody (i.e., anti-DA IgG antibody or anti-DNP IgE antibody, 3 nM) preincubated with a fixed concentration of small target analytes (i.e., Domoic Acid or DNP).

RESULTS AND DISCUSSION

Engineering Programmable DNA-Switches for Small Molecule Detection. The method we propose for the detection of small molecules (i.e., antigen) is based on the use both of synthetic DNA strands and a small molecule-binding antibody. Such DNA strands are able to generate two distinct DNA modules (a reporter and an input module, Figure 1A). The reporter module consists of a stem-loop DNA-probe (DNA-switch) labeled with a fluorophore/quencher pair with a single-stranded tail appended to one end, and a complementary DNA strand (Antigen-DNA) terminally labeled with a specific small molecule (i.e., antigen, purple hexagon, Figure 1A). The input module is composed of the same Antigen-DNA sequence

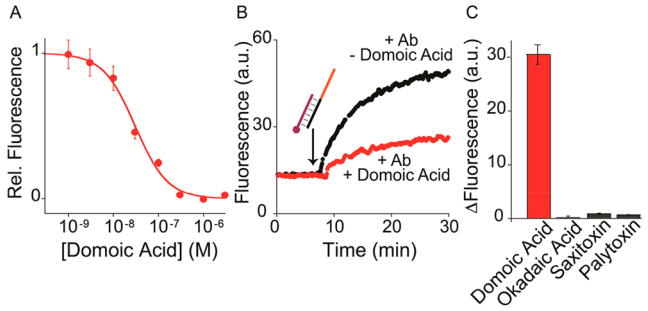

Figure 2. (A) Competitive DNA-based assay detects domoic acid at low nanomolar concentrations ($K_{1/2}$ = 30 ± 4 nM) in seawater sample. (B) Fluorescence kinetics showing the binding of the DA-input module (10 nM) to the DA-reporter module (10 nM) in a solution containing a fixed amount of anti-DA antibodies (3 nM) in the absence (black curve) and in the presence of saturating concentration of domoic acid (i.e., 3 μM, red curve). (C) The competitive DNA-based assay is specific and it does not exhibit any significant response at the presence of other marine toxins (i.e., 3 μM). All the reported values represent the average of at least three measurements and error bars reflect standard deviations. All the experiments were performed in 100 μL marine water at 35 °C.

that is also able to hybridize with a complementary DNA input strand containing a 15-base sequence complementary to the loop sequence of DNA-switch (orange portion in Figure 1A), and a second 40-base tail (black portion in Figure 1A) that allows high affinity binding with the Antigen-DNA strand. This modular design allows for simultaneous efficient coupling of Antigen-DNA strand both with the DNA-switch (to generate a reporter module) and the input strand (input module), while supporting their binding with the specific small molecule-binding antibody. Of note, the DNA-switch and the complementary input strand are rationally engineered in a way that their relative affinity binding is poor. Co-localization of the reporter and input modules on the same antibody brings the two elements into close proximity, thereby increasing their local concentrations. This binding event triggers the hybridization of the DNA-switch with the input strand which results in the consequent increase of the fluorescence output. The presence of small target molecules competing for the same antibody binding prevents the reporter and input modules to be in close proximity which leads to a decreased fluorescence emission. Our sensing strategy thus takes advantage of the difference in the binding affinity of a DNA-switch for its complementary DNA input strand when the two DNA elements are either free in solution (low binding affinity) or brought into close proximity by a specific small molecule-binding antibody (improved binding affinity).

Antibody-Mediated DNA-Based Platform for Domoic Acid and DNP Detection. To achieve proof of principle demonstration of the method, we selected domoic acid (DA) as a molecule of interest. Domoic acid is a marine neurotoxin produced by marine diatoms of the genus *Pseudonitzschia* during harmful algal blooms. This toxin enters food webs through feeding interactions and can accumulate in higher trophic levels, resulting in human[51] and marine mammal deaths.[52] Therefore, it is of high relevance to develop easy, sensitive, and low cost devices that can rapidly and continuously measure toxin levels at the point-of-need (PON). We also make use of a domoic acid-labeled DNA strand (DA-DNA) which hybridizes with both DNA-switch and

DOI: 10.1021/acs.analchem.8b01584
Anal. Chem. 2018, 90, 8196−8201

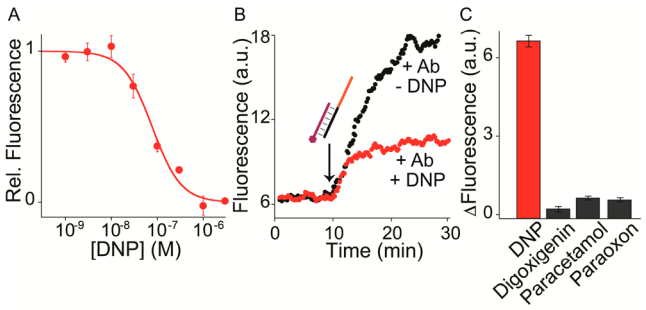

Figure 3. (A) Quantitative fluorescence detection of DNP displays detection range at low nanomolar concentrations ($K_{1/2}$ = 30 ± 4 nM) in tap water sample. (B) Fluorescence kinetics showing hybridization of the DNP-input module (10 nM) to the DNP-reporter module (10 nM) in a solution containing a fixed amount of anti-DNP antibodies (3 nM) in the absence (black curve) and in the presence of saturating concentration of DNP (i.e., 3 μM, red curve). (C) The DNP-sensing platform is highly specific and shows no significant response at the presence of other small target analytes (i.e., 3 μM). All the reported values represent the average of at least three measurements and error bars reflect standard deviations. All the experiments were performed in 100 μL seawater sample at 35 °C.

input strand to generate DA-reporter module and DA-input module, respectively. To elucidate the relationship between switching thermodynamics and signaling of the DA-reporter module, we have first designed a set of three variants of DNA-switch that retain a common 15-base loop and a 20-base tail complementary to the DA-DNA strand but differing in the GC content of the 5-base stem (Variant 1GC, 3GC, and 5GC, Figure 1B). Such variants differ in the stability of their off-states (Figure 1B). Specifically, by increasing the number of bases in the double-stranded stem we obtained variants with estimated free energies ranging from −0.96 kcal mol^{-1} to −5.48 kcal mol^{-1} (values predicted using *mfold* prediction software).[53] The stability of the on-state in contrast is effectively identical in all three variants (predicted stability ΔG = −1.39 kcal mol^{-1}).

This difference between the off- and on-states of the three variants, in turn, provides a means of controlling the dynamic range of the input strand concentration over which it binds the DNA-switch.[54,55] As expected, binding curves obtained at a fixed concentration of DA-reporter module (DNA switch + DA-DNA, 10 nM) with increasing concentrations of DA-input module (DA-DNA + input strand) indicate that the dynamic range of the input module concentration depends strongly on the GC-content of the stem ($K_{1/2\ 1GC}$ = 2.3 ± 0.2 nM; $K_{1/2\ 3GC}$ = 41 ± 3 nM; $K_{1/2\ 5GC}$ = 255 ± 19 nM) (black curves in Figures 1C and S1).

In the presence of saturating concentration of anti-DA antibodies (i.e., 100 nM), we observed an improvement of the binding affinity of the input module for all the three tested variants of DNA-switch ($K_{1/2\ 1GC}$ = 1.4 ± 0.1 nM; $K_{1/2\ 3GC}$ = 5.3 ± 0.7 nM; $K_{1/2\ 5GC}$ = 6.6 ± 0.6 nM, colored curves in Figure 1C), 1.6-folds for the variant 1GC, 7.7-folds for the 3GC and 38.6-folds for the 5GC, respectively. Binding of the anti-DA antibody to the recognition element of DA-DNA strand definitely leads the loop of DNA-switch and the complementary portion of input strand to stand into close proximity, thus improving their relative binding affinity and leading to an increase of the observed fluorescence signal. The largest improvement of binding affinity in the presence of anti-DA antibodies has been obtained for variant 5GC (Figures 1C and S2), which has been thus selected for the successive experiments.

To achieve optimal sensitivity of the competitive assay for small molecules detection, we first optimized the concentration of the DA-input module that leads to the largest difference in antibody-induced difference in occupancy at its lowest possible concentration (10 nM, Figure 1D). Second, we performed binding curves by adding increasing concentration of the DA-input module to the DA-reporter module in the presence of a fixed amount of anti-DA antibodies (i.e., 100 nM) and domoic acid (ranging from 30 nM to 3 μM) in the same solution (Figure 1E, F). As a result, the linear dynamic range over which the DA-reporter module responds to the DA-input module is tuned as a function of domoic acid concentration (orange curves in Figure 1F). This demonstrates that the presence of free domoic acid in solution reduces the hybridization efficiency of the DA-reporter module with the DA-input module. This is essentially due to the competition for antibody binding sites between free domoic acid and domoic acid-labeled to DNA strand. As expected, the higher the concentration of free domoic acid, the lower binding affinity of the DA-input module for the DA-input module. Indeed, at saturating concentration of domoic acid the DA-input module shows an affinity binding for the DA-reporter module that is identical to that reported in the absence of anti-DA antibodies ($K_{1/2}$ = 270 ± 17 nM, Figures 1G and S3). We finally identified the optimal concentration of DA-DNA strand and anti-DA antibody to set up the fluorescence competitive assay. To do this, we have performed binding curves in the presence of a fixed concentration of DA-reporter and DA-input modules by adding increasing concentrations of anti-DA antibodies. As a result, the system responds rapidly to anti-DA antibodies generating a 500% fluorescence signal gain at saturating concentration of anti-DA antibodies achieving a detection limit in the low nanomolar range ($K_{1/2}$ = 2.2 ± 0.2 nM, Figure S4). Accordingly, we also selected the optimal concentration of antibody for the competitive assay (i.e., 3 nM) and the minimal concentration of DA-DNA strand required to achieve the highest sensitivity in the competitive format (i.e., 10 nM, Figure S5). To further support the principle of method, we then performed control experiments to confirm that the detection of anti-DA antibodies is highly selective and no significant signal change occurs in the presence of nonspecific antibodies (Figure S6).

Finally, we test the platform for the single-step detection of domoic acid in a buffer solution (Figure S7) and in marine water samples (Figure 2). Detection of domoic acid is achieved by adding the DA-reporter (10 nM) and DA-input modules (10 nM) into a solution containing domoic acid previously preincubated with anti-DA antibodies (3 nM, 10 min of incubation). This platform is sensitive enough to allow for domoic acid detection at low nanomolar concentration (detection limit of 7 ± 2 nM, Figure 2A). Of note, the difference of ionic strength between the buffer solution and the marine water samples slightly changes the relative signal gain of the sensing platform without affecting the binding affinities (K_{D_buffer} = 40 ± 5 nM; $K_{D\_seawater}$ = 32 ± 5 nM; Figure S8). Fluorescence kinetics showing the hybridization rates of DA-input module with DA-reporter module in the absence and in the presence of saturating concentration of domoic acid (i.e., 3 μM) indicate that our platform is also rapid and reaches the equilibrium in about 20 min. The platform produces a higher change in fluorescence emission in this condition, consistent with the fact that the two modules can bind the same anti-DA

DOI: 10.1021/acs.analchem.8b01584
Anal. Chem. 2018, 90, 8196−8201

antibody in the absence of target domoic acid (black curve, Figure 2B) and come into close proximity. However, the system responds in the same time frame also at saturating concentration of domoic acid (red curve, Figure 2B). Finally, we tested the selectivity of the sensing platform, and we observed no significant cross reactivity in the presence of other related marine toxins (Figure 2C).

Although our method could not reach the sensitivity of other approaches based on the amplification step such as, for example, the commercially available enzyme-linked immunosorbent assay (ELISA, 10-fold lower sensitivity), we note that the performances of our single-step platform for DA detection present important features such as modularity, rapid response, and high specificity that make the methodology extremely versatile.[56] In this regard, the modularity of our platform allows, in principle, for detecting any small target molecule that can be conjugated to a DNA strand. To highlight this feature, we have tested a different compound (i.e., 2,4-dinitrophenol, DNP) labeled to the same DNA sequence to produce a DNP-labeled DNA strand. This modular approach allows single-step measurement of DNP concentration directly in tap water by simply changing the antigen-labeled DNA strand (Figure 3). Of note, DNP is one the most toxic and refractory pollutant, widely used in manufacturing of pesticides, pharmaceuticals, and explosive materials and categorized as a priority pollutant.[57]

Our DNP sensor displays a linear dynamic range from 30 nM to 200 nM, a limit of detection (LOD) of 20 ± 3 nM (Figure 3A), and the same features in terms of response time and specificity to those observed with the domoic acid platform (Figure 3B and C). This confirms the flexibility and versatility of the proposed strategy, with a detection mechanism potentially adaptable to the measurement of any small molecule.

CONCLUSIONS

Herein, we designed and developed a modular, highly versatile, and cost-effective DNA-based sensing platform to detect environmentally relevant small molecules in water sample (i.e., marine and tap water) in few minutes and without washing steps. We engineered fluorescence structure-switching DNA-based probes whose affinity for their complementary single stranded DNA sequence can be regulated as a function of small molecules and their cognate antibodies concentration. The simultaneous binding of DNA elements with the antibody results in an increase of the local concentration of the probes which definitely triggers their hybridization and the consequent increase of fluorescence signal. Competition between small target molecules free in solution and those labeled to the DNA strand for binding sites of the antibody provides a means to quantify small target molecules concentration in a homogeneous competitive format. We thus demonstrated that our fluorescence sensing platform can efficiently detect in a single-step measurement different small target molecules with high sensitivity (low nanomolar levels), good specificity, and rapid response time directly in sea and tap water samples. In conclusion, we point out that this method could, in principle, be generalized to the detection of any small molecule that can be conjugated to a DNA strand and for which a specific antibody is available. Besides the rapid response and high specificity discussed above, the method is reagentless and is suitable for multiplexed detection of different small target molecule. The same sensing strategy can also be extended to other output signals (i.e., electrochemical or UV−vis), thus making the platform even more suitable for real-time in situ monitoring of small molecules. Besides applications in on field environmental analysis, this DNA-based immunoassay displays attributes that make it suitable for the rapid screening of small target molecules and for point-of-care analysis in clinical applications.

ASSOCIATED CONTENT

Supporting Information

The Supporting Information is available free of charge on the ACS Publications website at DOI: 10.1021/acs.analchem.8b01584.

Data analysis and supporting Figures (PDF)

AUTHOR INFORMATION

Corresponding Author

*Email: alessandro.porchetta@uniroma2.it. (A.P.)

ORCID

Alessandro Porchetta: 0000-0002-4061-5574

Author Contributions

All authors have given approval to the final version of the manuscript.

Notes

The authors declare no competing financial interest.

ACKNOWLEDGMENTS

This work was supported by the European Union's Seventh Framework Programme for research, technological development, and demonstration under grant agreement no. 613844.

REFERENCES

(1) Altenburger, R.; Scholz, S.; Schmitt-Jansen, M.; Busch, W.; Escher, B. I. *Environ. Sci. Technol.* **2012**, *46*, 2508−2522.

(2) Scott, D. E.; Bayly, A. R.; Abell, C.; Skidmore, J. *Nat. Rev. Drug Discovery* **2016**, *15*, 533−550.

(3) Devillier, P.; Salvator, H.; Naline, E.; Couderc, L.-J.; Grassin-Delyle, S. *Curr. Pharm. Des.* **2017**, *23*, 2050−2059.

(4) Butcher, R. A. *Nat. Chem. Biol.* **2017**, *13*, 577−586.

(5) Rotariu, L.; Lagarde, F.; Jaffrezic-Renault, N.; Bala, C. *TrAC, Trends Anal. Chem.* **2016**, *79*, 80−87.

(6) Gałuszka, A.; Migaszewski, Z. M.; Namieśnik, J. *Environ. Res.* **2015**, *140*, 593−603.

(7) Soler, L.; Sánchez, S. *Nanoscale* **2014**, *6*, 7175−7182.

(8) Yager, P.; Domingo, G. J.; Gerdes, J. *Annu. Rev. Biomed. Eng.* **2008**, *10*, 107−144.

(9) Yetisen, A. K.; Akram, M. S.; Lowe, C. R. *Lab Chip* **2013**, *13*, 2210−2251.

(10) Kumar, A. A.; Hennek, J. W.; Smith, B. S.; Kumar, S.; Beattie, P.; Jain, S.; Rolland, J. P.; Stossel, T. P.; Chunda-Liyoka, C.; Whitesides, G. M. *Angew. Chem., Int. Ed.* **2015**, *54*, 5836−5853.

(11) Yan, X.; Li, P.; Zhou, B.; Tang, X.; Li, X.; Weng, S.; Yang, L.; Liu, J. *Anal. Chem.* **2017**, *89*, 4875−4881.

(12) Kahraman, M.; Mullen, E. R.; Korkmaz, A.; Wachsmann-Hogiu, S. *Nanophotonics* **2017**, *6*, 831−852.

(13) Brennwald, M. S.; Schmidt, M.; Oser, J.; Kipfer, R. *Environ. Sci. Technol.* **2016**, *50*, 13455−13463.

(14) Zenobi, R. *Science* **2013**, *342*, 1243259−1243259.

(15) Schwartzman, O.; Tanay, A. *Nat. Rev. Genet.* **2015**, *16*, 716−726.

(16) Xia, Y.; Si, J.; Li, Z. *Biosens. Bioelectron.* **2016**, *77*, 774−789.

(17) Au, A. K.; Huynh, W.; Horowitz, L. F.; Folch, A. *Angew. Chem., Int. Ed.* **2016**, *55*, 3862−3881.

(18) Li, Q.; Chen, P.; Fan, Y.; Wang, X.; Xu, K.; Li, L.; Tang, B. *Anal. Chem.* **2016**, *88* (17), 8610−8616.

DOI: 10.1021/acs.analchem.8b01584
Anal. Chem. 2018, 90, 8196−8201

(19) Estevez, M. C.; Alvarez, M.; Lechuga, L. M. *Laser Photon. Rev.* **2012**, *6*, 463−487.
(20) López-Marzo, A. M.; Merkoçi, A. *Lab Chip* **2016**, *16*, 3150−3176.
(21) Liu, X.; Freeman, R.; Golub, E.; Willner, I. *ACS Nano* **2011**, *5*, 7648−7655.
(22) Ricci, F.; Vallée-Bélisle, A.; Simon, A. J.; Porchetta, A.; Plaxco, K. W. *Acc. Chem. Res.* **2016**, *49*, 1884−1892.
(23) Vallée-Bélisle, A.; Ricci, F.; Plaxco, K. W. *J. Am. Chem. Soc.* **2012**, *134*, 2876−2879.
(24) Lee, M. H.; Kim, J. S.; Sessler, J. L. *Chem. Soc. Rev.* **2015**, *44*, 4185−4191.
(25) Del Grosso, E.; Idili, A.; Porchetta, A.; Ricci, F. *Nanoscale* **2016**, *8*, 18057−18061.
(26) Vallée-Bélisle, A.; Ricci, F.; Uzawa, T.; Xia, F.; Plaxco, K. W. *J. Am. Chem. Soc.* **2012**, *134*, 15197−15200.
(27) Idili, A.; Amodio, A.; Vidonis, M.; Feinberg-Somerson, J.; Castronovo, M.; Ricci, F. *Anal. Chem.* **2014**, *86*, 9013−9019.
(28) Lin, M.; Song, P.; Zhou, G.; Zuo, X.; Aldalbahi, A.; Lou, X.; Shi, J.; Fan, C. *Nat. Protoc.* **2016**, *11*, 1244−1263.
(29) Pei, H.; Lu, N.; Wen, Y.; Song, S.; Liu, Y.; Yan, H.; Fan, C. *Adv. Mater.* **2010**, *22*, 4754−4758.
(30) Swensen, J. S.; Xiao, Y.; Ferguson, B. S.; Lubin, A. A.; Lai, R. Y.; Heeger, A. J.; Plaxco, K. W.; Soh, H. T. *J. Am. Chem. Soc.* **2009**, *131*, 4262−4266.
(31) Pelossof, G.; Tel-Vered, R.; Elbaz, J.; Willner, I. *Anal. Chem.* **2010**, *82*, 4396−4402.
(32) Schoukroun-Barnes, L. R.; Macazo, F. C.; Gutierrez, B.; Lottermoser, J.; Liu, J.; White, R. J. *Annu. Rev. Anal. Chem.* **2016**, *9*, 163−181.
(33) Soh, J. H.; Lin, Y.; Rana, S.; Ying, J. Y.; Stevens, M. M. *Anal. Chem.* **2015**, *87*, 7644−7652.
(34) Li, J.; Fu, H. E.; Wu, L. J.; Zheng, A. X.; Chen, G. N.; Yang, H. H. *Anal. Chem.* **2012**, *84*, 5309−5315.
(35) Ma, X.; Chen, Z.; Kannan, P.; Lin, Z.; Qiu, B.; Guo, L. *Anal. Chem.* **2016**, *88*, 3227−3234.
(36) Wang, J.; Zhu, G.; You, M.; Song, E.; Shukoor, M. I.; Zhang, K.; Altman, M. B.; Chen, Y.; Zhu, Z.; Huang, C. Z.; Tan, W. *ACS Nano* **2012**, *6*, 5070−5077.
(37) Tan, W.; Donovan, M. J.; Jiang, J. *Chem. Rev.* **2013**, *113*, 2842−2862.
(38) Kashefi-Kheyrabadi, L.; Mehrgardi, M. A.; Wiechec, E.; Turner, A. P. F.; Tiwari, A. *Anal. Chem.* **2014**, *86*, 4956−4960.
(39) Iliuk, A. B.; Hu, L.; Tao, W. A. *Anal. Chem.* **2011**, *83*, 4440−4452.
(40) Imaizumi, Y.; Kasahara, Y.; Fujita, H.; Kitadume, S.; Ozaki, H.; Endoh, T.; Kuwahara, M.; Sugimoto, N. *J. Am. Chem. Soc.* **2013**, *135*, 9412−9419.
(41) McKeague, M.; Derosa, M. C. *J. Nucleic Acids* **2012**, *2012*, 1−20.
(42) Porter, E. B.; Polaski, J. T.; Morck, M. M.; Batey, R. T. *Nat. Chem. Biol.* **2017**, *13*, 295−301.
(43) Zuo, X.; Xiao, Y.; Plaxco, K. W. *J. Am. Chem. Soc.* **2009**, *131*, 6944−6945.
(44) Ageely, E. A.; Kartje, Z. J.; Rohilla, K. J.; Barkau, C. L.; Gagnon, K. T. *ACS Chem. Biol.* **2016**, *11*, 2398−2406.
(45) Filonov, G. S.; Moon, J. D.; Svensen, N.; Jaffrey, S. R. *J. Am. Chem. Soc.* **2014**, *136*, 16299−16308.
(46) You, M.; Litke, J. L.; Jaffrey, S. R. *Proc. Natl. Acad. Sci. U. S. A.* **2015**, *112*, E2756−E2765.
(47) Mahshid, S. S.; Ricci, F.; Kelley, S. O.; Vallée-Bélisle, A. *ACS Sensors* **2017**, *2*, 718−723.
(48) Harroun, S. G.; Prévost-Tremblay, C.; Lauzon, D.; Desrosiers, A.; Wang, X.; Pedro, L.; Vallée-Bélisle, A. *Nanoscale* **2018**, *10*, 4607−4641.
(49) Cheng, S.; Shi, F.; Jiang, X.; Wang, L.; Chen, W.; Zhu, C. *Anal. Chem.* **2012**, *84*, 2129−2132.
(50) Porchetta, A.; Ippodrino, R.; Marini, B.; Caruso, A.; Caccuri, F.; Ricci, F. *J. Am. Chem. Soc.* **2018**, *140*, 947−953.
(51) Lefebvre, K. A.; Robertson, A. *Toxicon* **2010**, *56*, 218−230.
(52) Scholin, C. A.; Gulland, F.; Doucette, G. J.; Benson, S.; Busman, M.; Chavez, F. P.; Cordaro, J.; DeLong, R.; De Vogelaere, A.; Harvey, J.; Haulena, M.; Lefebvre, K.; Lipscomb, T.; Loscutoff, S.; Lowenstine, L. J.; Marin, R., III; Miller, P. E.; McLellan, W. A.; Moeller, P. D. R.; Powell, C. L.; Rowles, T.; Silvagni, P.; Silver, M.; Spraker, T.; Trainer, V.; Van Dolah, F. M. *Nature* **2000**, *403*, 80−84.
(53) Zuker, M. *Nucleic Acids Res.* **2003**, *31*, 3406−3415.
(54) Adornetto, G.; Porchetta, A.; Palleschi, G.; Plaxco, K. W.; Ricci, F. *Chem. Sci.* **2015**, *6*, 3692−3696.
(55) Vallée-Bélisle, A.; Ricci, F.; Plaxco, K. W. *Proc. Natl. Acad. Sci. U. S. A.* **2009**, *106*, 13802−13807.
(56) Saeed, A. F.; Awan, S. A.; Ling, S.; Wang, R.; Wang, S. *Algal Res.* **2017**, *24*, 97−110.
(57) Puig, D.; Barceló, D. *TrAC, Trends Anal. Chem.* **1996**, *15*, 362−375.

DOI: 10.1021/acs.analchem.8b01584
Anal. Chem. 2018, 90, 8196−8201